Observations of marine atmospheric boundary layer transitions across the summer Kuroshio Extension

Youichi TANIMOTO[1,2], Shang-Ping XIE[3,4] , Kohei KAI[1],
Hideki OKAJIMA[4,2], Hiroki TOKINAGA[6,3], Toshiyuki MURAYAMA[5],
Masami NONAKA[2], and Hisashi NAKAMURA [7,2]

[1]Graduate School of Environmental Science/Faculty of Environmental Earth Science, Hokkaido University, Sapporo, Japan

[2]Frontier Research Center for Global Change, Japan Agency for Marine-Earth Science and Technology, Yokohama, Japan

[3]International Pacific Research Center, SOEST, University of Hawaii, Honolulu, HI

[4]Department of Meteorology, SOEST, University of Hawaii, Honolulu, HI

[5]Faculty of Marine Technology, Tokyo University of Marine Science and Technology, Tokyo, Japan

[6]Institute for Observational Research for Global Change, Japan Agency for Marine-Earth Science and Technology, Yokosuka, Japan

[7]Department of Earth and Planetary Science, University of Tokyo, Tokyo, Japan

Submitted to *Journal of Climate*

December 29, 2007

Revised June 10, 2008

Revised September 9, 2008

Accepted October 3, 2008

Corresponding Author address:

Youichi Tanimoto

Faculty of Environmental Earth Science

Hokkaido University

N10 W5, Kita-ku, Sapporo 060-0810, Japan

E-mail: tanimoto@ees.hokudai.ac.jp

Abstract

The Baiu and Kuroshio Extension (KE) fronts, both zonally oriented and nearly collocated east of Japan, are the dominant summertime features of the atmosphere and ocean, respectively, over the mid-latitude Northwest Pacific. An atmospheric sounding campaign was conducted on R/V *Roger Revelle* during the 2005 summer. Transects of soundings across the KE front are analyzed to study its effects on the atmosphere, along with continuous surface-meteorological and ceilometer cloud-base observations. While the KE front remained nearly stationary during the cruise, the Baiu front displayed large meridional displacements that changed wind direction across the KE front. The presence of sharp sea surface temperature (SST) gradients anchored by the KE enhanced the thermal and moisture advection, causing substantial changes in the marine atmospheric boundary layer (MABL) structure. When the Baiu front was displaced north of the KE front, southwesterly winds advected warm, humid air from the subtropics over the cold water, producing a surface inversion in favor of fog formation. When the Baiu front was to the south, on the other hand, northerly winds across the KE front destabilized the MABL, leading to the formation of a solid low-cloud deck beneath a strong capping inversion. The wind changes with the meridional displacement of the Baiu front thus caused large variations in near-surface atmospheric stability and surface turbulent heat fluxes, with potential feedback on deep convection and fog/low-cloud formation around the front.

1. Introduction

Over the Northwest Pacific east of the Japanese main island Honshu, sea surface temperature (SST) exhibits rich structures associated with the Kuroshio Extension (KE) meanders and pinched-off meso-scale eddies between the northern edge of the subtropical gyre and Kuroshio-Oyashio Interfrontal Zone (see Figure 1 in Yasuda et al. 1996). The narrow KE jet displays larger decadal variability (Nonaka et al. 2006; Taguchi et al. 2007) in response to basin-scale changes in surface wind curls (Schneider and Miller 2001; Qiu 2003). Strong ocean advection and the deep winter mixed layer allow subsurface variability to affect SST (Xie et al. 2000; Tomita et al. 2002) and surface heat flux (Tanimoto et al. 2003). Strong SST gradients east of Japan maintain baroclinicity in the marine atmospheric boundary layers (MABL), which has been suggested as important for atmospheric storm tracks (Inatsu et al. 2003; Nakamura et al. 2004). While most studies of the Kuroshio-atmosphere interaction have so far been based on models or model-assimilated analyses, in-situ vertical soundings of the atmosphere have been lacking, hampering the progress in characterizing and understanding the KE's influence on the atmosphere.

Tokinaga et al. (2006) conducted Global Positioning System (GPS) sonde soundings over the KE region onboard research vessels during the 2003/04 winter. They report strong modulations of the atmospheric mixed layer by synoptic weather disturbances. The atmospheric mixed layer was found to develop as high as 1500 m with reduced vertical wind shear in response to the northerly cold advection across the KE front, in association with the passage of cold fronts. The southerly warm advection, by contrast, was found to suppress the mixed layer development with strong vertical wind shear. These results support that the mixed layer adjustment to changes in near-surface atmospheric stability causes positive correlation between SST and wind speed around the KE front (Nonaka and Xie 2003) and other extratropical SST fronts as observed by satellite microwave measurements (see recent reviews by Xie 2004, Chelton et al. 2004, and Small et al. 2008).

During the 2005 summer we have carried out a similar atmospheric sounding campaign onboard research vessel (R/V) *Roger Revelle* over the KE region, complemented by continuous laser ceilometer and surface meteorological measurements. Drastically different from winter, the summer climate over the KE region is characterized by a convective rain

band called the Baiu/Meiyu front and by an extensive low-cloud deck to the north that occupies the entire midlatitude/subpolar North Pacific (Klein and Hartmann 1993; Norris 1998b). This low-cloud deck displays large temporal variability that is important for maintaining low-frequency SST anomalies during summer (Zhang et al. 1998; Norris 2000; Mochizuki and Awaji 2008).

Figure 1 depicts distributions of SST, surface winds and rainfall observed during our summer survey. In our study area (black box), the KE anchors a zonal SST front just east of Tokyo (35-36^{o}N), with SST decreasing from 23 to 20^{o}C just over ~100 km across the front. The Baiu/Meiyu rain band extends from eastern China through our study area into the North Pacific with a general northeastward tilt. Southwesterly surface winds converge from the south onto the rain band where the subtropical warm/moist and subpolar cool/dry air masses meet. In our study area, a precipitation band and the associated strong surface southwesterlies tend to be confined to the warmer flank of the quasi-steady KE front, suggestive of an SST influences.

The present study reports on the results from the cruise survey during the 2005 summer over the KE region, where strong SST fronts are featured along the KE as well as to the north and south. To our knowledge, this is the first successful atmospheric sounding campaign under the summer Baiu front across the KE front. As pointed out by Ninomiya (1984), the Baiu/Meiyu front over the East China Sea is characterized by pronounced meridional gradient of humidity rather than of temperature, while the front east of Japan accompanies strong meridional gradient not only of humidity but also of temperature. Our KESS cruise thus offers a unique opportunity to study the nature of interaction between the Baiu and KE fronts. As a first step, we focus on the effects of the KE front on the MABL structure including low clouds. On monthly mean, the atmospheric Baiu front was roughly collocated with the KE front in our study region, but the former displayed strong variability on the synoptic timescale. We show that the MABL experienced major changes as the atmospheric Baiu front moved north and south of the quasi-stationary KE front in the ocean. While using soundings taken for a short period, mechanisms discussed in the present study may operate for the climatology and decadal variability near the KE front.

In the rest of the paper, Section 2 describes the field campaign and data. Section 3

describes the synoptic ocean and atmospheric conditions during the campaign and presents the observations results in vertical sections across the KE front. Section 4 discusses the implications for the Baiu. Section 5 is a summary and discussion.

2. Observations and data

As part of the Kuroshio Extension System Study (KESS; Donohue et al. 2008), a joint survey of the ocean-atmosphere system (KESS-05) was conducted from 17 June 2005 through 16 July 2005 over the KE and Kuroshio recirculation (the black rectangle in Fig. 1) onboard R/V *Roger Revelle* of the Scripps Institution of Oceanography. The present study focuses on two meridional transects of the atmospheric soundings across the KE front completed within slightly more than three days to illustrate the MABL modulation by the oceanic front. Figures 2a and 2b show the sounding stations (green X marks) along the transects overlaid on the concurrent SST field (colors). These two transects are chosen for detailed analysis because they are geographically close but representing contrasting atmospheric conditions characterized by the southwesterly and northerly winds, respectively, at the surface. The first transect took 1.5 days to complete (Fig. 2a; hereafter Line A) with eleven (11) soundings, starting from the cold flank of the meandering KE front at Station A1 (36.56^{o}N, 146.88^{o}E) at 0510 UTC 11 July 2005 onto the warm flank at Station A11 (34.37^{o}N, 145.99^{o}E) at 1846 UTC 12 July 2005 (hereafter Period A). Consisting of six (6) GPS soundings, the second transect (Fig. 2b; Line/Period B) west of Line A started half day later from the warm flank of the KE front at Station B1 (34.83^{o}N, 144.10^{o}E) at 0741 UTC 13 July 2005 onto the cold flank at Station B6 (36.70^{o}N, 144.83^{o}E) at 0733 UTC 14 July 2005.

Onboard the ship, we used GPS sondes of the latest type (Vaisala RS92-SGP) to measure air temperature, relative humidity (RH), pressure and wind velocity every two seconds from the sea surface to about 20 km in the lower stratosphere. The sonde data were transmitted to an onboard receiver (Vaisala Digicora III of the Shigaraki Middle and Upper Atmosphere Observatory, Kyoto University) and then linearly interpolated to vertical intervals of 10m. We use the data from the surface to 4.0 km height to study the MABL.

Cloud base was continuously monitored at 1-minute intervals with a ceilometer (Vaisala CT25K of Tokyo University of Marine Science and Technology) mounted on top of the

bridge. In each measurement, the ceilometer emitted a train of pulsed laser beam vertically and records the averaged backscattered signal for 12 s. Then the ceilometer automatically reported cloud base heights up to three detected by a build-in algorithm as well as the backscatter profile (Kahn et al. 2004, Vaisala Oj 1999).

Surface marine meteorological observations of SST, surface air temperature (SAT), surface wind velocity, relative humidity (RH), rainfall, and solar radiation are available at 1-minute intervals. We use 60-minute running averages except for RH. Since RH records contain some spike-like noises, we use the original records at 1-minute intervals. As a measure of static stability near the surface, parameter S = SST-SAT is calculated. Positive (negative) values of S indicate the unstable (stable) near-surface atmosphere. Steep SST changes of 4.2^{o}C and 3.1^{o}C are recorded across Lines A and B, respectively.

To capture synoptic conditions of the ocean and atmosphere during the KESS-05 cruise, we employ the AMSR-E (Advanced Microwave Scanning Radiometer for Earth Observing System) SST and rainfall products from Remote Sensing Systems, available in 3-day running mean on a 0.25^{o} grid; and the Quick scatterometer (QuikSCAT) surface wind vector product, available at weekly intervals on a 0.25^{o} grid (Liu et al., 2000).

We also use the meso-scale operational weather analysis (M-ANAL) for the Far East (20-50^{o}N, 120-150^{o}E) provided by the Japan Meteorological Agency (JMA), including wind velocity, temperature, and RH in the lower troposphere (975, 950, 925, 900, 800, and 700 hPa), available at 6-hour intervals on a 0.25^{o} longitude by 0.20^{o} latitude grid. The sounding data from the KESS-05 cruise were not assimilated into the M-ANAL system.

3. MABL modifications across the KE SST front

a. Synoptic conditions of the ocean and atmosphere

During the three-day period for Lines A and B, SST (colors in Fig. 2a) displays a steep front along 36^{o}N with a cold meander and a cold ocean eddy centered at 36^{o}N, 146^{o}E. The eddy was about 1^{o} x 1^{o} longitude-latitude in diameter. Line A was nearly meridional (Fig. 2a) and cut across the cold eddy located just to the north of the KE front, while Line B was located west of the eddy but cut across the SST front of KE (Fig. 2b). As expected from a large heat capacity of the ocean, SST was nearly the same during Periods A and B.

During the three-day period, the Baiu front stretched over several thousand kilometers from the lower Yangtze River in eastern China through Japan into the western North Pacific. A close look into the JMA surface weather maps indicates that the Baiu front was located north of the KE front during Period A (Fig. 3a) and then displaced to its south during Period B (Fig. 3b). As displayed in the satellite infrared (IR) images, Line A (Fig. 3c) was overlaid by high-level clouds (i.e., lower cloud top temperatures) extending southwestward from the surface low at 44^{o}N, 152^{o}E along the Baiu front, while Line B (Fig. 3d) was under low-level clouds (higher cloud top temperatures) prevailing to the north of the Baiu front.

In association with the southward shift of the Baiu front from Period A to B, the lower atmosphere on the KE SST front at 35^{o}N 145^{o}E experienced rapid changes (Fig. 2c). Specifically, the M-ANAL shows a large decrease in equivalent potential temperature (θ_e) by 8 K, a rapid deceleration of the southwesterly wind by 15 ms^{-1} and a sign reversal of the meridional wind component from 1200 UTC to 1800 UTC 12 July 2005, indicating that the Baiu front passed this location sometime in this period. Therefore, the sounding location of A9 (34.95^{o}N at 0424 UTC 12 July) was still a little south of the Baiu front, while the last two soundings of A10 (34.70^{o}N at 1421 UTC 12 July) and A11 (34.37^{o}N at 1846 UTC 12 July) along Line A were affected by disturbances in the Baiu front as described later. For Period B, the Baiu front was always located south of Line B. Though the Baiu front was nearby, surface rainfall was not reported on board the ship in either transect. Consistently, none of the seven AMSR-E snapshots for Periods A and B indicates any precipitation in the sounding area (not shown).

During Period A prior to these rapid changes, surface winds were southwesterly and convergent across a meridional maximum of θ_e at 850 hPa ($\theta_{e@850}$) that was associated with moist air on the southern flank of the Baiu front (Fig. 2a). This is rather similar to the monthly mean conditions in Fig. 1a. As a result of warm/moist advections by the southwesterlies, $\theta_{e@850}$ was high ranging from 337 to 342K over Line A (contours in Fig. 2a). On the first day of Period B (0000 to 1800 UTC 13 July 2005), surface winds turned northerly over the KE SST front, with high $\theta_{e@850}$ (>340 K) displaced to the south (Fig. 2b). On Line B, $\theta_{e@850}$ decreased by 10 K to 327-333K.

Meridional displacements of the Baiu front relative to the stationary KE front, via the

associated changes in surface advection of temperature and humidity, brought about large changes in the MABL, as described in the rest of this section.

b. Line A under surface southwesterlies

Figure 4 displays observations along Line A, which cut through the cold ocean eddy (35.5-36.1^{o}N), then the steep SST front of KE (35.2-35.3^{o}N), and finally arrived in a warm pool south of 35.2^{o}N. The SST front of KE was quite strong, with SST changing by 4^{o}C in less than 20 km (~35.25^{o}N). The corresponding meridional gradient of SAT was much more relaxed, varying only by 4^{o}C over ~90 km (from 36.0^{o}N to 35.2^{o}N) as opposed to an SST change of 7^{o}C on Line A. The SAT profile is consistent with the warm advection by the southerlies, with the near-surface atmosphere nearly in equilibrium with underlying SST on the upwind side of the SST front and in rather slow adjustment to the rapid decrease in SST on its downwind side. As a result, the near-surface stratification was nearly neutral (-0.5 > S > -1.7^{o}C) on the warmer flank of the KE front, while it was strongly stable (S < -4^{o}C) on the colder flank of the front and over the cold eddy (blue curve in Fig. 4c). (Small ripples on the surface variable records are due to stops made for ocean hydrographic observations, each lasting for a few hours.)

Figure 5 shows a sounding in the near-neutral regime (Station A9 at ~34.95^{o}N) on the warmer flank of the KE front (gray curves). It features a surface mixed layer and major inversion at 1100 m. In between there were two minor inversions at 300 m and at 550 m. Figure 4a shows that a surface mixed layer with nearly uniform virtual potential temperature developed over the near-neutral regime on the warmer flank of the KE front (A8-A9) and stratification was still weak above the mixed layer top (at ~300 m) up to the bottom of the main inversion (at 1100 m or above). The greater turbulent mixing in the MABL over the near-neutral regime is indicated by a decrease in surface RH (Fig. 4c) and a slight increase in surface wind speed (Fig. 4d) in the section between A8 and A9 relative to the other sections north of A7 and south of A10. In 34.8-35.6^{o}N, the ceilometer measurements identified a double cloud base at around 400 m and 1100 m, corresponding to the top of the mixed layer and the main inversion base, respectively (Fig. 4a). In fact, the histogram of cloud base heights for a 6-hour period (a total of 360 ceilometer samples) just south of the KE front

(35.20^{o} to 34.92^{o}N; gray bars in Fig. 6) clearly shows double peaks in layers between 300 and 500 m and between 1000 and 1200 m. The histogram in Fig. 6 also indicates that there were some occasions when the ceilometer detected no cloud base. During this daytime period (0900-1500 Local Time, 12 Jul 2005), the on-board pyranometer recorded 591 Wm^{-2} of solar radiation on average with its standard deviation of 190 Wm^{-2}, and the radiation fluctuated between over 1000 Wm^{-2} and below 300 Wm^{-2}. It was partly sunny at A8 according to our field note. These results suggest the formation of scattered stratocumulus and/or shallow cumulus in the MABL on the warmer flank of the KE front in the presence of warm/moist southerly winds. These cloud types are climatologically prevalent in this region during summer (Norris 1998b).

As mentioned in Section 3a, the southward-moving Baiu front at the surface was probably close to the ship at sounding locations of A10 and A11. The surface southerlies observed on the ship mean that the Baiu front at the surface was still to the north. The movement of the Baiu front may cause variations in vertical structure among the soundings south of the KE front. The increase in surface wind speed, decrease in surface relative humidity, and increase in cloud base height for A7-A9 all seem consistent with greater turbulent mixing in the MABL. A strong inversion develops at 1100 m, above which the free troposphere is dry. The soundings A10 and A11, by contrast, observe higher relative humidity up to higher levels at 1800m as well as at the bottom of the MABL probably due to meso-α features associated with the Baiu front nearby.

To the north of Station A8, a thin surface inversion formed as the southwesterly winds carried warm and moist air across the KE front over the cold ocean surface (Fig. 4a). In this stable regime, both surface sensible and latent heat fluxes were downward because SAT and surface specific humidity were higher than SST and surface saturated specific humidity, respectively (Figs. 4b and 4e). Figure 5 displays a typical sounding at Station A4 (black curves). The surface inversion was about 150 m thick. The atmosphere was saturated from the surface to 800 m, indicating the formation of a thick fog layer. Dew point temperature in the lower MABL was nearly uniform meridionally between A4 (black dashed line in Fig. 5) and further upwind (e.g., at A9: gray dashed line in Fig. 5), while air temperature at A4 was typically cooler by 2-3^{o}C. The formation of strong surface stratification accompanying

overcastting fog under southerlies has been reported in the composited soundings at the ocean weather station C in the subpolar North Atlantic (Norris 1998a).

Figure 5 thus suggests that the fog formation was facilitated by the cooling of warm and moist air through heat exchanges with the cool ocean, as it crossed the oceanic front. In fact, both on the cold flank of the KE front and over the cold ocean eddy, the fog formation was recognized by visual observations and confirmed by ceilometer measurements of cloud base height (Fig. 4a). A histogram of the cloud base height thus measured for 6-hour periods over the strongly stable regime from 36.35^{o} to 35.88^{o}N (black bars in Fig. 6) shows the predominance of a near-surface mode with the average cloud base at 35m. Norris (1998b) has pointed out that the formation of a surface inversion and associated fog are due to warm, moist airflow across an SST front towards the cooler side, as confirmed by our transect observations. Whereas the climatological frequency of fog occurrence is rather low (~5%) south of 40^{o}N in the western North Pacific (Norris 1998b), cloud type composites by Norris and Iacobellis (2005) show that the warm, moist southerlies across the SST front over the North Pacific favor the fog formation.

The onsets of the surface inversion layer and surface humidity saturation (RH=100) were almost coincidental, occurring at A8 (35.2^{o}N) and at 35.25^{o}N between A8 and A7, respectively (Figs. 4a and 4c), whereas the grounding of the ceilometer-measured cloud base occurred further downwind to the north of A6 (35.7^{o}N). This delay must be due either to the presence of a fog layer that was too thin to be detected by the ceilometer or to strong surface wind speed south of A6. Wind speed dropped rapidly from more than 10 ms^{-1} at A8 to about 5 ms^{-1} at A5 (Fig. 4d), resulting from the suppressed vertical mixing of wind momentum within the MABL due to the rapid decrease in SST and the resultant stabilization of the near-surface atmosphere (Nonaka and Xie 2003; Tokinaga et al. 2006). The suppressed turbulent mixing within the MABL favors fog formation. Similar formation (break-up) of sea fog were observed on the colder (warmer) flank of the KE front on 4-5 July 2005 during the same cruise, though the transition was not as clear as in Fig. 4.

c. Line B under surface northerlies

Along Line B, SST (blue curve in Fig. 7b) displayed a steep front in 35.4-36.0^{o}N

between nearly uniform warm and cold pools. As evident in Fig. 7d, northeasterly winds of 3-5 ms^{-1} prevailed during the first half of the 24-hour transect, while southeasterlies of 3-5 ms^{-1} dominated during its second half. The northeasterlies brought cold air from the colder flank of the KE front, and the southeasterlies for the second half of Period B still advected cooler air from the region of the cold ocean eddy located southeast of the transect (Fig. 2b). The northeasterly cool advection was anomalous compared to the climatological southwesterlies during the Baiu season in this region (Fig. 1). Correspondingly, the SAT profile was characteristic of cold advection (Fig. 7b), nearly in equilibrium with SST on the colder flank and adjusting slowly to the rapid SST increase on the front and its warmer flank. The SAT gradient was thus more relaxed than the SST gradient across the transit of Line B (red curve in Fig. 7b). As a result, the near-surface stratification was close to being neutral or slightly unstable ($-0.1 < S < 0.5^{o}$C) on the colder flank of the SST front, while it was strongly unstable ($1.5 < S < 2.5^{o}$C) on its warmer flank. Correspondingly, surface sensible heat flux was upward to the south of the SST front, while it was diminished to its north. Nevertheless, Fig. 7e suggests that surface latent heat flux was upward on either side of the SST front under the unsaturated cool air, though enhanced over the warmer water. These upward heat fluxes along Line B under the cool advection were in sharp contrast to the downward fluxes along Line A with strong warm advection.

Line B was located north of the Baiu front, where the MABL was topped by low clouds with their base at 400-800 m under a strong inversion at the 1000 m level (Fig. 7a). Above the inversion RH was typically around 50%, while it exceeded 90% in the MABL above the mixed layer top at 600-700 m. In this moist layer, the ceilometer detected cloud base that was elevated south of the SST front relative to its north (800 m versus 600 m).

Immediately above the inversion, virtual potential temperature was almost uniform meridionally (Fig. 7a). Thus, the variations in the MABL temperature (from 298 to 295K) observed along Line B must reflect the effect of the SST front. Moving from the north across the SST front, we observed the inversion base elevated by 100 m and RH right underneath increased by 10%, likely due to the enhanced surface heat fluxes and vertical mixing on the warmer flank of the front. This rise in the inversion base due to the cool advection on the warm flank of the SST front is consistent with a mixed-layer model proposed by Schubert et

al. (1979). In their experiment of cool advection toward warm SST, a gradual SST increase accompanies a deepening of the MABL associated with enhanced heat supply from the ocean.

Figure 8 compares vertical profiles of air temperature and dew point between Stations B3 and B4. At Station B3 (south of the SST front in the unstable surface regime), a layer between 700 and 900 m was saturated with moisture (gray curves in Fig. 8), indicating cloud formation below the main inversion. At Station B4 (north of the SST front in the near-neutral surface regime; black curves in Fig. 8), the lapse rate was about $6^{o}C(km)^{-1}$ in a layer between 600 and 750 m below the main inversion. It was close to the moist adiabatic lapse rate, suggestive of cloud formation in that nearly saturated layer (Fig. 7) as detected by the ceilometer (Fig. 7a). Owing to the reduced vertical mixing over low SST, the MABL at Station B4 was more strongly stratified than at B3. On the poleward flank of the SST front, higher RH in the cooler surface mixed layer probably helped lower the cloud base as observed.

The lower cloud base north of the KE front relative to its south is evident also in the time-height section of ceilometer backscatter intensity measured at 1-minute intervals (Fig. 9a). As the ship was traveling northward across the intense SST front during the 60-minute period of 1930-2030 UTC 13 July 2005 (blue curve in Fig. 9b), the height of the upper boundary of strong backscatter [red shade > 1.0 $x10^{-2}$ km^{-1} sr^{-1}] showed a 200-m decrease from 650-800 m to 450-600 m. Especially during 1600-1930 UTC in the unstable surface regime on the warmer flank of the SST front, the layer of high backscatter was very steady in altitude, indicating full overcast with a flat cloud base. In the near-neutral surface regime on the colder flank of the front, by contrast, the high backscatter layer displayed much larger vertical displacements. This feature is indicative of the presence of thin clouds without a solid cloud base on the colder flank of the SST front, where a cloud base was sometimes identified below 400 m. When this happened, a second cloud base was detected at 600 m, close to the level at which single cloud bases are identified. Sporadic, weak backscatters of 0.05-0.1 $x10^{-2}$ km^{-1} sr^{-1} (blue shade in Fig. 9a) spread in a wider vertical range, sometimes reaching all the way to the surface, indicating drizzles. Indeed, no surface rainfall was observed on the ship.

Figure 9c compares histograms of the ceilometer cloud base height between the unstable and near-neutral surface regimes. As in Fig. 6, totally 360 (6 hours) samples are used for each of the regimes. In a manner consistent with Fig. 9a, the cloud base height tends to be lower in

the near-neutral regime than in the unstable regime, at 583 m and 749 m on average, respectively, and its standard deviation is larger in the near-neutral regime (114 m) than in the unstable regime (66 m). Occasionally in the near-neutral surface regime, no cloud base was identified (Fig. 9c). These ceilometer statistics confirm the prevalence of broken, scattered clouds in the near-neutral surface regime on the colder flank of the SST front and that of a solid low-cloud deck in the unstable surface regime on its warmer flank.

4. MABL structure in and outside the Baiu front

Along the subtropical flank of the Baiu front, there is a rain band that often accompanies a deep moist layer, as detected by several soundings on Line A. Thus, the Baiu front separates a moist, subtropical air mass from a drier, subpolar air mass to the north. Figure 10a compares a moist, subtropical profile based on a sounding at A6 and a drier, subpolar profile based on a sounding at B3. These two soundings conducted roughly at the same latitude (35.6^{o}N) are chosen to avoid latitudinal biases. The underlying SST was 17^{o}C at A6 (at the center of the cold eddy) and 23.5^{o}C at B3.

The sounding A6 indicates that two layers of 0-1700 m and 4500-6100 m were almost saturated, in which temperature roughly followed the moist adiabatic profile punctuated by six inversions at 4500, 2600, 1700, 1200, 600 and 100 m levels. All these inversions except the one near the surface were weak and likely to be caused by the differential advection of temperature and moisture. In contrast, the near-surface inversion formed as the warm tropical air blew across the SST front onto the cold eddy, as discussed earlier. High moisture contents in Sounding A6 were maintained by the southwesterly advection of a moist, subtropical air (Fig. 10b) that became saturated probably due to a weak synoptic ascent associated with the Baiu front. In fact, satellite IR image indicates relatively high clouds at around A6 (not shown). In contrast, the subpolar sounding at B3 indicates a much drier condition below 3500m, where moisture was trapped mostly in the MABL with a thin cloud layer between 600 and 900 m capped by a strong inversion. A significant increase in dew point at 3500 m on a sounding at B3 indicates that the subtropical air mass still remained in the mid-troposphere. Indeed, the meridional winds were northerly in a layer of 4800-6500 m but still southerly aloft.

The sharp contrasts in temperature, moisture and cloud distributions between the two soundings are mainly caused by the synoptic meridional displacement of the Baiu front. As the subtropical or subpolar air mass is being advected across the SST front, strong adjustments take place in the MABL as reflected in surface turbulent heat flux and vertical structures of temperature, moisture and cloud. Meridional thermal advection is important in the MBAL where large temperature differences (4-6^{o}C) are observed between Periods A and B. It is interesting to note that because of strong warm advection, the MABL is much warmer at A6 than B3, despite a much lower SST at the former station (17 vs. 23.5^{o}C). Importance of the meridional advection is also manifested as a more pronounced difference in MABL dew point temperature between A6 and B3.

5. Summary and discussion

We have analyzed atmospheric in-situ observations on the KESS-05 summer cruise to study the effects of the KE front on the MABL. The data include GPS sonde soundings, and continuous observations of surface meteorological variables and cloud base height with a laser ceilometer. These in-situ data are complemented with a suite of satellite observations and an operational meso-scale atmospheric analysis. The Baiu and KE fronts are the dominant summertime features of the atmosphere and ocean in the region, respectively. The KE front remained quite stationary during our study period, while the Baiu front moved substantially north and south on the synoptic weather timescale, accompanying sign reversals of the meridional component of surface winds. The presence of the strong SST front anchored by the KE enhances the effects of thermal and moisture advection by meridional winds, causing substantial changes in the MABL structure. The effects of the KE front on the MABL are illustrated with two cross-frontal transects.

Line A sampled the Baiu front, with a few soundings capturing a deep moist layer with temperatures nearly in the moist-adiabatic lapse rate. Robust southwesterly winds prevailed at the surface on Line A. As warm, humid subtropical air moved across the KE front onto cold water to the north, a surface inversion and a thick fog layer formed. The MABL stratification was highly stable, with downward surface sensible heat flux on the colder flank of the SST front. On the warmer flank, by contrast, the MABL stratification was nearly neutral, and

stratocumulus (or shallow cumulus) clouds formed with elevated cloud base heights of either 300-600 m (the top of the surface mixed layer) or ~1000 m (bottom of the main inversion).

Measurements along Line B were carried out after the Baiu front had moved away to the south, sampling the subpolar air mass with a strong inversion capping a moist MABL. Moderate northeasterlies prevailing north of the Baiu front advected the cold subpolar air across the KE front to the south. In this circumstance, the MABL stratification was highly unstable, activating surface turbulence to enhance heat and moisture supply from the warm ocean. The associated intensification of vertical mixing led to the deepening of the MABL and moistening of its upper portion where a solid cloud deck formed below the inversion. A sharp transition was observed across the KE front. Over the cooler ocean north of the front, the cloud deck was replaced with broken clouds scattering with lower cloud base. Under the almost neutral or stable stratification in the MABL, suppressed vertical mixing of moisture was unfavorable for maintaining a solid cloud deck near the MABL top. Similar modulations of low clouds can be found over a meandering SST front over the eastern equatorial Pacific (Deser et al. 1993; Hashizume et al. 2001).

Changes in thermal advection associated with meridional migration of the Baiu front can exert different effects on the near-surface and free atmosphere. Under the southerly warm advection, the near-surface stratification is strongly stable, but the high moisture content advected from the south forms a deep moist layer in the free atmosphere. The northerly advection of cool, dry air, on the other hand, destabilizes the MABL stratification while suppressing deep convection. The presence of the quasi-stationary SST front along KE substantially can strengthen the aforementioned advective effects. On Line A, for example, enhanced advection of warm, moist air from the south, once across the SST front, increased the surface stability over the cool ocean surface. A surface inversion and sea fog formed, shutting off surface evaporation that would otherwise moisten the MABL and increase convective instability.

Surface latent heat flux around the KE front observed in our survey varied from zero under the moist southerlies (Line A) to 120 Wm^{-2} under the drier northerlies (Line B). This and other possible effects of the KE front on the Baiu front and associated cloud formation and precipitation need further investigations. Unlike the observed cross sections, the vertical

gradient of the M-ANAL virtual potential temperature is found much more uniform within the lower troposphere, failing to represent the inversions near the surface and at the top of the mixed layer along Lines A and B, respectively. With further improvement of numerical models, continuous monitoring of atmospheric and oceanic conditions and the subsequent improvement in the quality of (meso-scale) analysis data, we could deepen our understanding of the mechanisms of decadal SST anomalies in the oceanic frontal zone along the KE and Oyashio Extension observed in conjunction with variability in low-level cloud cover (Norris 2000) and into decadal changes observed recently in heat release from Kuroshio with possible impact on the Baiu-frontal precipitation (Tomita et al. 2007).

Acknowledgments

We wish to thank Prof. Randy Watts, the chief scientist of the KESS-05 cruise, the captain and crew of R/V *Roger Revelle* for support for atmospheric soundings, G. Takagaki, M. Roxy and A. Goto for their participation in the cruise survey. Drs. M. Yamamoto and J. Furumoto of the Shigaraki Middle and Upper Atmosphere Observatory, Kyoto University kindly lent us the sounding system and provided practical advices on the usage. Advice from Dr. K. Ishikawa, the Ocean Research Institute, University of Tokyo and Prof. Y. Fujiyoshi, the Institute of Low Temperature Science, Hokkaido University, was helpful in executing our observations. This work was supported in part by Grand-In-Aid for Scientific Research defrayed by the Ministry of Education, Culture, Sports, Science and Technology of Japan (17340137, 15340153 and 18204044), the Sumitomo Foundation (043426), the Japan Agency for Marine-Earth Science and Technology, the U.S. National Science Foundation and National Aeronautic and Space Administration. YT conducted this work at IPRC, University of Hawaii on a sabbatical leave from Hokkaido University. IPRC publication Number 553 and SOEST publication Number 7566. Graphic outputs were made by use of the GrADS.

References

Chelton, B. D., M. G. Schlax, M. H. Freilich, and R. F. Milliff, 2004: Satellite measurements reveal persistent small-scale features in ocean winds. *Science*, **303**, 978-983.

Deser, C., J. J. Bates, and S. Wahl, 1993: The influence of sea surface temperature on stratiform cloudiness along the equatorial front in the Pacific Ocean. *J. Climate*, **6,** 1172-1180.

Donohue, K. A., and Coauthors, 2008: Program studies the Kuroshio Extension. *EOS*, **89**, 161-162.

Kahn R., and co-authors, 2004: Environmental snapshots from ACE-Asia, *J. Geophys. Res*., **109**, D19S14, doi:10.1029/2003JD004339.

Hashizume, H., S.-P. Xie, W.T. Liu and K. Takeuchi, 2001: Local and remote atmospheric response to tropical instability waves: A global view from the space. *J. Geophys. Res.-Atmos*., **106**, 10173-10185.

Inatsu, M., H. Mukougawa, and S.-P. Xie, 2003: Atmospheric response to zonal variations in mid-latitude SST: Transient and stationary eddies and their feedback. *J. Climate*, **16**, 3314-3329.

Klein, S. and D. L. Hartmann 1993: The seasonal cycle of low stratiform clouds. *J. Climate*, **6**, 1587–1606.

Liu, W. T., X. Xie, P. S. Polito, S.-P. Xie, and H. Hashizume, 2000: Atmospheric manifestation of tropical instability waves observed by QuikSCAT and Tropical Rain Measuring Mission. *Geophys. Res. Lett*., **27**, 2545–2548.

Mochizuki, T. and T. Awaji, 2007: Summertime evolution of decadal sea surface temperature anomalies in the midlatitude North Pacific. *J. Climate*, 21, 1569-1588.

Nakamura, H., T. Sampe, Y. Tanimoto, A. Shimpo, 2004: Observed associations among storm tracks, jet streams and midlatitude oceanic fronts. "Earth's Climate: The Ocean-Atmosphere Interaction", C. Wang, S.-P. Xie, J. A. Carton, Eds., Geophys. Monogr., 147, American Geophysical Union, Washington, D.C., U.S.A., 329-346.

Ninomiya, K., 1984: Characteristics of Baiu front as a predominant subtropical front in the summer Northern Hemisphere. *J. Meteor. Soc. Japan*, **62**, 880-894.

Nonaka, M. and S.-P. Xie, 2003: Covariations of sea surface temperature and wind over the

Kuroshio and its extension: evidence for ocean to atmosphere feedback. *J. Climate*, **16**, 1404-1413.

Nonaka, M., H. Nakamura, Y. Tanimoto, T. Kagimoto, H. Sasaki, 2006: North Pacific decadal variability in SST and frontal structure simulated in a high-resolution OGCM. *J. Climate*, **19**, 1970-1989.

Norris, J. R., 1998a: Low cloud type over the ocean from surface observations. Part I: relationship to surface meteorology and the vertical distribution of temperature and moisture. *J. Climate*, **11**, 369-382.

Norris, J. R.,1998b: Low cloud type over the ocean from surface observations. Part II: geographical and seasonal variations. *J. Climate*, **11**, 383-403.

Norris, J. R., 2000: Interannual and interdecadal variability in the storm track, cloudiness, and sea surface temperature over the summertime North Pacific. *J. Climate*, **13**, 422-430.

Norris, J. R., and S. F. Iacobellis, 2005: North Pacific cloud feedbacks inferred from synoptic-scale dynamic and thermodynamic relationships. *J. Climate*, **18**, 4862-4878.

Qiu, B., 2003: Kuroshio Extension variability and forcing of the Pacific Decadal Oscillations: Responses and potential feedback. *J. Phys. Oceanogr.*, **33**, 2465–2482.

Schubert, W.H., J.S. Wakefield, E.J. Steiner and S. K. Cox, 1979: Marine stratocumulus convection. Part II: horizontally inhomogeneous solutions. *J. Atmos. Sci.*, **36**, 1308-1324.

Schneider, N. and A. Miller, 2001: Predicting western North Pacific Ocean climate. *J. Climate*, **14**, 3997–4002.

Small, R.J., S. deSzoeke, S.-P. Xie, L. O'Neill, H. Seo, Q. Song, P. Cornillon, M. Spall, and S. Minobe, 2008: Air-sea interaction over ocean fronts and eddies. *Dynam. Atmos. Ocean.*, Accepted.

Taguchi, B., S.-P. Xie, N. Schneider, M. Nonaka, H. Sasaki, and Y. Sasai, 2007: Decadal variability of the Kuroshio Extension: Observations and an eddy-resolving model hindcast. *J. Climate*, **20**, 2357–2377.

Tanimoto, Y., H. Nakamura, T. Kagimoto, S. Yamane, 2003: An active role of extratropical sea surface temperature anomalies in determining anomalous turbulent heat flux. *J. Geophy. Res.*, **108**(C10), 3304, doi: 10.1029/2002JC001750.

Tokinaga, H., Y. Tanimoto, M. Nonaka, B. Taguchi, T. Fukamachi, S.-P. Xie, H. Nakamura, T. Watanabe and I. Yasuda, 2006. Atmospheric sounding over the winter Kuroshio Extension: effect of surface stability on atmospheric boundary layer structure. *Geophys. Res. Lett.*, **33**, L04703, doi: 10.1029/2005GL025102.

Tomita, T., S.-P. Xie and M. Nonaka, 2002: Estimates of surface and subsurface forcing for decadal sea surface temperature variability in the mid-latitude North Pacific. *J. Meteor. Soc. Japan*, **80**, 1289-1300.

_____, H. Sato, M. Nonaka, and M. Hara, 2007: Interdecadal variability of the early summer surface heat flux in the Kuroshio region and its impact on the Baiu frontal activity. *Geophy. Res. Lett.*, **34**, L10708, doi: 10.1029/2007GL029676.

Vaisala Oj, 1999: Ceilometer CT25K User's Guide, CT25K-U059en-2.1.

Xie, S.-P., T. Kunitani, A. Kubokawa, M. Nonaka and S. Hosoda, 2000: Interdecadal thermocline variability in the North Pacific for 1958-1997: A GCM simulation. *J. Phys. Oceanogr.*, **30**, 2798-2813.

Xie, S.-P., 2004: Satellite observations of cool ocean-atmosphere interaction. *Bull. Amer. Meteor. Soc.*, **85**, 195–208.

Yasuda, I., K. Okuda and Y. Shimizu, 1996: Distribution and modification of the North Pacific Intermediate Water in the Kuroshio-Oyashio Interfrontal zone. *J. Phys. Oceanogr.*, **26**, 448-465.

Zhang, Y., J.R. Norris and J.M. Wallace, 1998: Seasonality of large-scale atmosphere-ocean interaction over the North Pacific. *J. Climate*, **11**, 2473-2481.

Figure captions

Figure 1: AMSR-E SST (contours at 1^{o}C intervals), rainfall (color shades in mm day^{-1}), and QuikSCAT surface winds (vectors in ms^{-1}) averaged during the KESS-05 cruise (17 June – 16 July, 2005). The inset rectangle indicates the study area of the cruise.

Figure 2: (a) AMSR-E SST in 3-day running mean centered on 11 July 2005 (color shades in ^{o}C), equivalent potential temperature at 850 hPa (contours at 1K intervals) and surface winds (vectors at ms^{-1}) from M-ANAL averaged for the first day of Period A (from 0600 UTC 11 to 0000 UTC 12 July 2005. (b) Same as in (a), but for Period B (13 July 2005 for SST and from 0000 to 1800 UTC 13 July for M-ANAL). Cross symbols in (a) and (b) indicate the sounding stations along Lines A and B, respectively. (c) Time-height section of equivalent potential temperature (color contours in K) and wind velocities (vectors at ms^{-1}) at 35^{o}N, 145^{o}E based on the M-ANAL.

Figure 3: JMA surface weather map on (a) 0000 UTC 11 July and (b) 0000UTC 13 July 2005, showing the analyzed Baiu front. The ship tracks, Lines A and B, are superimposed with heavy black lines in (a) and (b), respectively. (c, d) The corresponding infrared images of the GOES-9 satellite. The ship tracks are superimposed with heavy green lines. The satellite images are provided by Kochi University (http://weather.is.kochi-u.ac.jp/) and JMA.

Figure 4: (a) Latitude-height section of virtual potential temperature (black contours at 1K intervals) and relative humidity (RH; color shades in %) observed by GPS sondes along Line A. White dots denote the cloud base determined from the ceilometer. Shipboard marine meteorological observations along Line A: (b) SST (blue curve in ^{o}C) and SAT (red in ^{o}C); (c) SST-SAT (*S*; blue curve in ^{o}C), 100 minus surface RH (black dots in %); (d) surface zonal (black in ms^{-1}) and meridional (gray in ms^{-1}) wind velocities; (e) saturated specific humidity at the sea surface (blue in g kg^{-1}) and surface specific humidity (red in g kg^{-1}). Except RH, 60-minute running mean is shown. For RH, the original 1-minute interval is employed.

Figure 5: Vertical profiles of air temperature (solid curves in ^{o}C) and dew point (dashed in ^{o}C) at Stations A4 (black) and A9 (gray).

Figure 6: Histogram of ceilometer-detected cloud base height on Line A . Black (gray) bars

are for the strongly stable (near-neutral) surface regime. A total of 360 one-minute samples are used for each regime.

Figure 7: Same as in Fig. 4, but for Line B. Black dots in (c) represent 90 minus RH (%).

Figure 8: Same as in Fig. 5, but for Stations of B3 (gray) and B4 (black).

Figure 9: (a) Time-height section of ceilometer backscatter intensity [colors in 10^{-2} km^{-1} sr^{-1}] and primary cloud base (black dots). The second cloud base is plotted in gray dots when reported. (b) Time series of shipboard SST (blue in ^{o}C) and SAT (red in ^{o}C) from 1300 UTC 13 July to 0300 UTC 14 July 2005 when the ship was sailing from the warmer to colder flank of the KE SST front. (c) Same as in Fig. 6, but for Line B.

Figure 10: Vertical profiles of (a) air temperature (solid curves in ^{o}C) and dew point (dashed in ^{o}C), (b) meridional wind (solid curves in ms^{-1}) at Stations A6 (black) and B3 (gray).

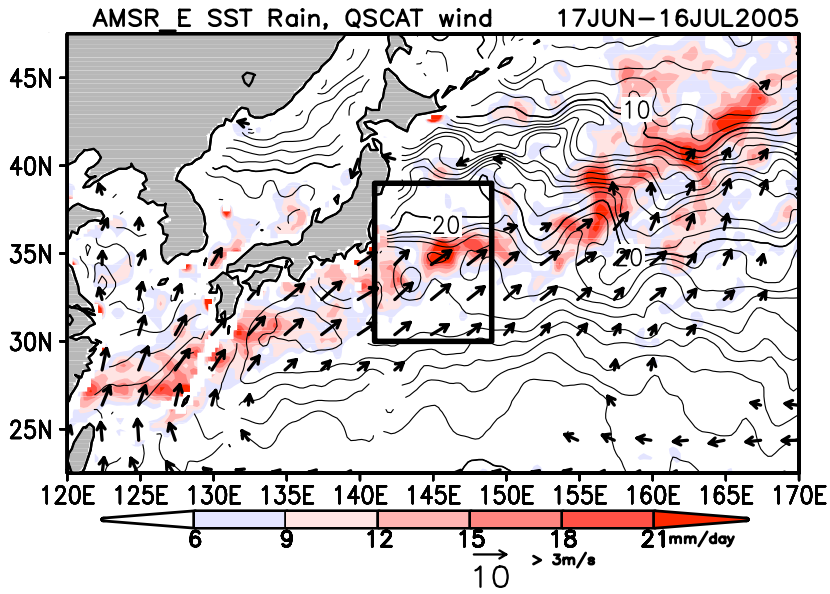

Figure 1: AMSR-E SST (contours at 1°C intervals), rainfall (color shades in mm day^{-1}), and QuikSCAT surface winds (vectors in ms^{-1}) averaged during the KESS-05 cruise (17 June – 16 July, 2005). The inset rectangle indicates the study area of the cruise.

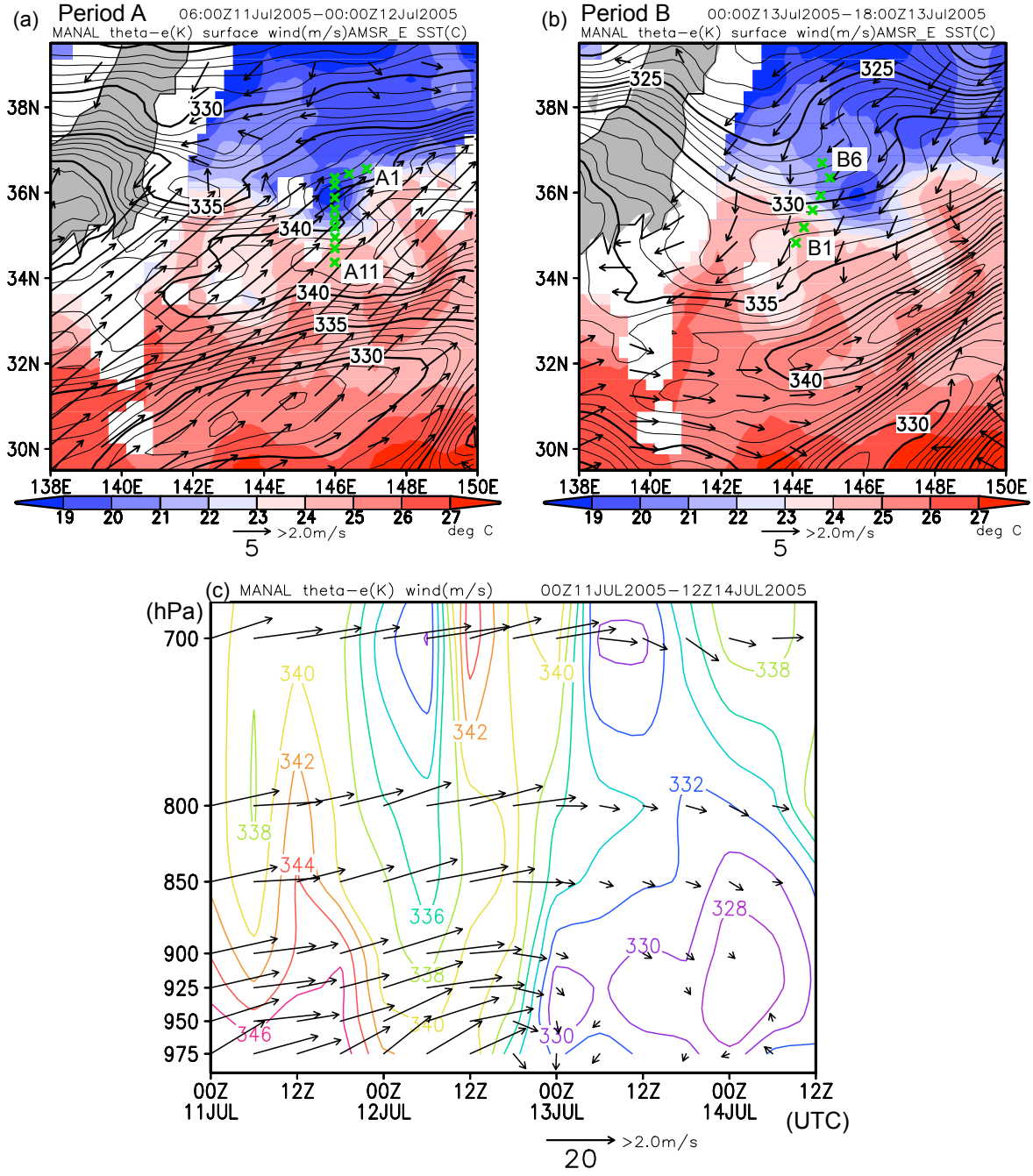

Figure 2: (a) AMSR-E SST in 3-day running mean centered on 11 July 2005 (color shades in ^{o}C), equivalent potential temperature at 850 hPa (contours at 1K intervals) and surface winds (vectors at ms^{-1}) from M-ANAL averaged for the first day of Period A (from 0600 UTC 11 to 0000 UTC 12 July 2005. (b) Same as in (a), but for Period B (13 July 2005 for SST and from 0000 to 1800 UTC 13 July for M-ANAL). Cross symbols in (a) and (b) indicate the sounding stations along Lines A and B, respectively. (c) Time-height section of equivalent potential temperature (color contours in K) and wind velocities (vectors at ms^{-1}) at 35^{o}N, 145^{o}E based on the M-ANAL.

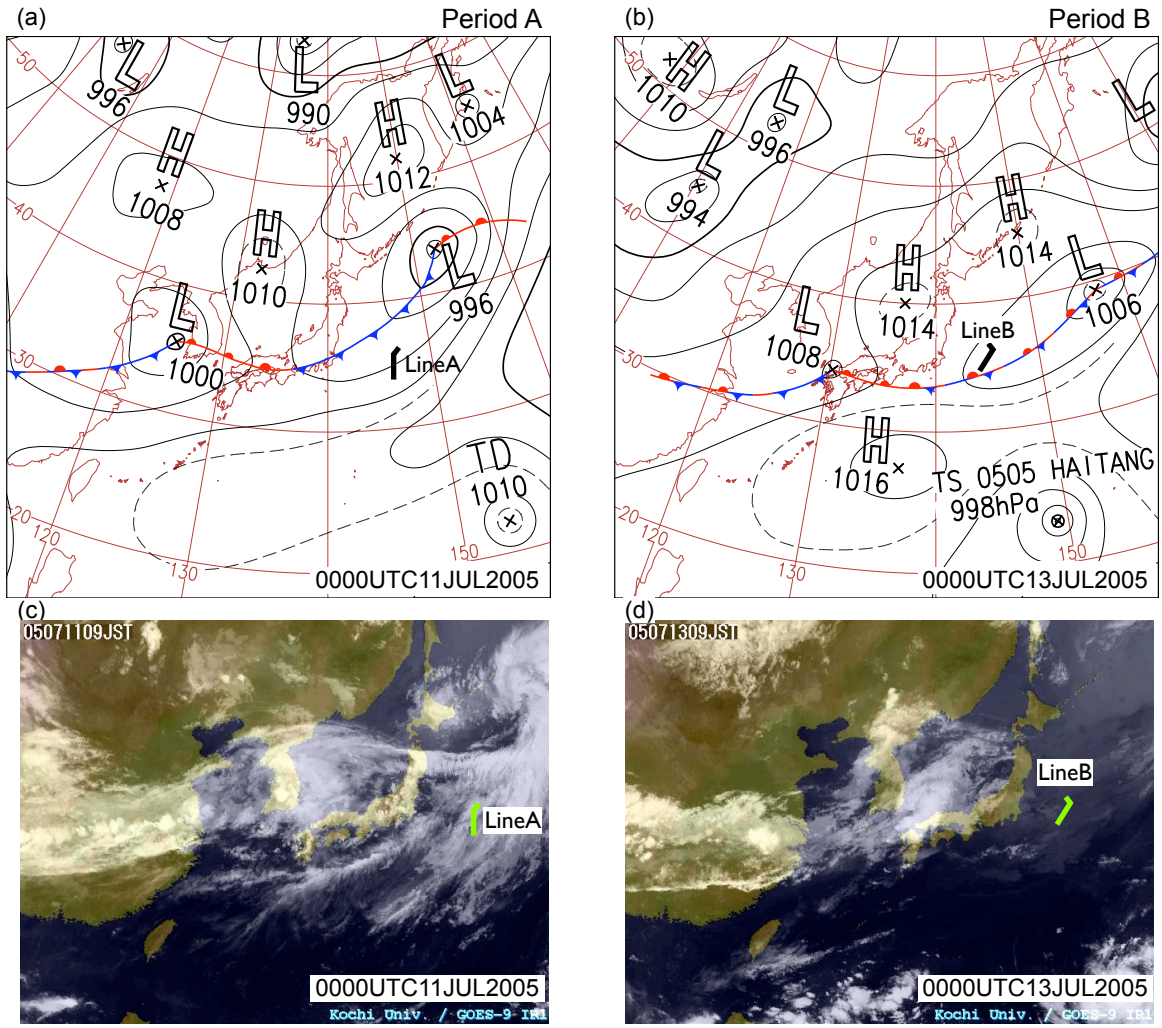

Figure 3: JMA surface weather map on (a) 0000 UTC 11 July and (b) 0000UTC 13 July 2005, showing the analyzed Baiu front. The ship tracks, Lines A and B, are superimposed with heavy black lines in (a) and (b), respectively. (c, d) The corresponding infrared images of the GOES-9 satellite. The ship tracks are superimposed with heavy green lines. The satellite images are provided by Kochi University (http://weather.is.kochi-u.ac.jp/) and JMA.

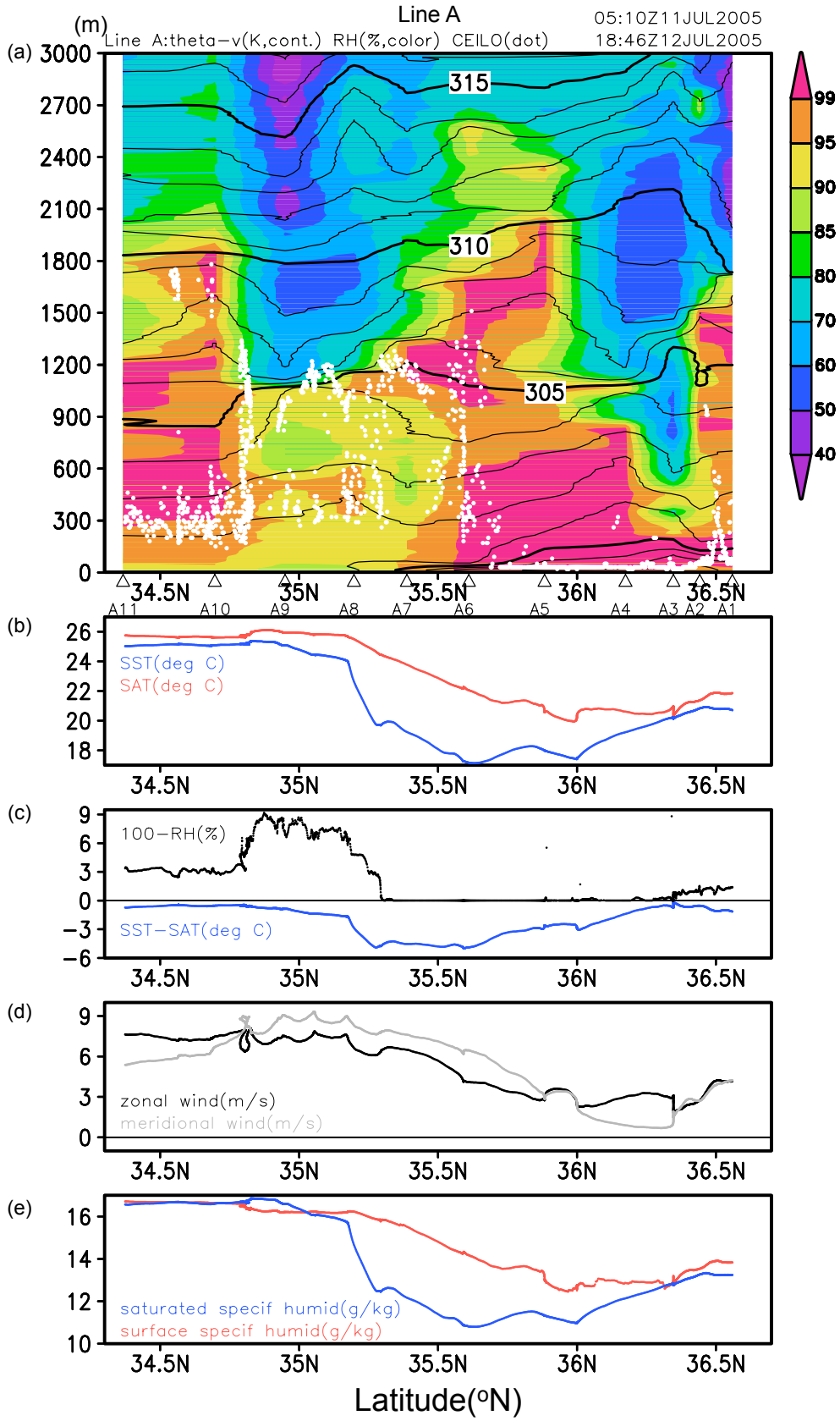

Figure 4: (a) Latitude-height section of virtual potential temperature (black contours at 1K intervals) and relative humidity (RH; color shades in %) observed by GPS sondes along Line A. White dots denote the cloud base determined from the ceilometer. Shipboard marine meteorological observations along Line A: (b) SST (blue curve in °C) and SAT (red in °C); (c) SST-SAT (*S*; blue curve in °C), 100 minus surface RH (black dots in %); (d) surface zonal (black in ms^{-1}) and meridional (gray in ms^{-1}) wind velocities; (e) saturated specific humidity at the sea surface (blue in g kg^{-1}) and surface specific humidity (red in g kg^{-1}). Except RH, 60-minute running mean is shown. For RH, the original 1-minute interval is employed.

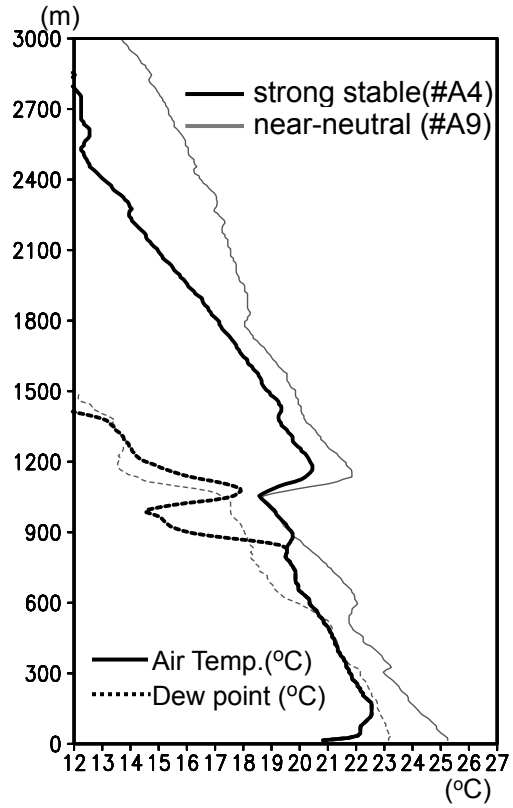

Figure 5: Vertical profiles of air temperature (solid curves in °C) and dew point (dashed in °C) at Stations A4 (black) and A9 (gray).

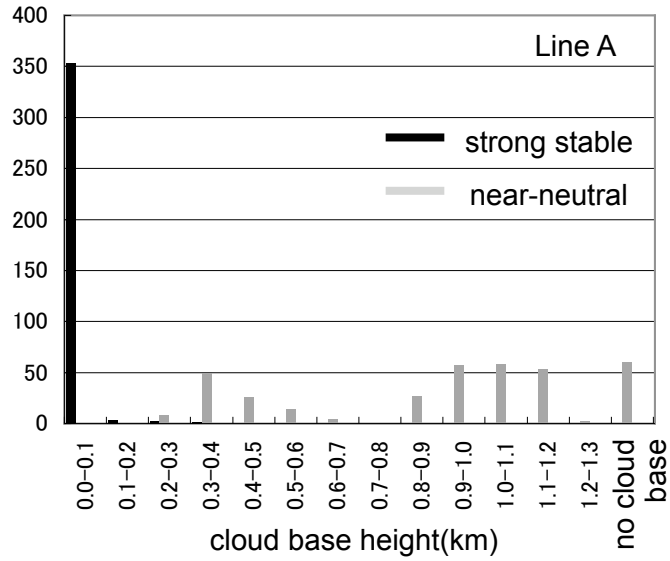

Figure 6: Histogram of ceilometer-detected cloud base height on Line A . Black (gray) bars are for the strongly stable (near-neutral) surface regime. A total of 360 one-minute samples are used for each regime.

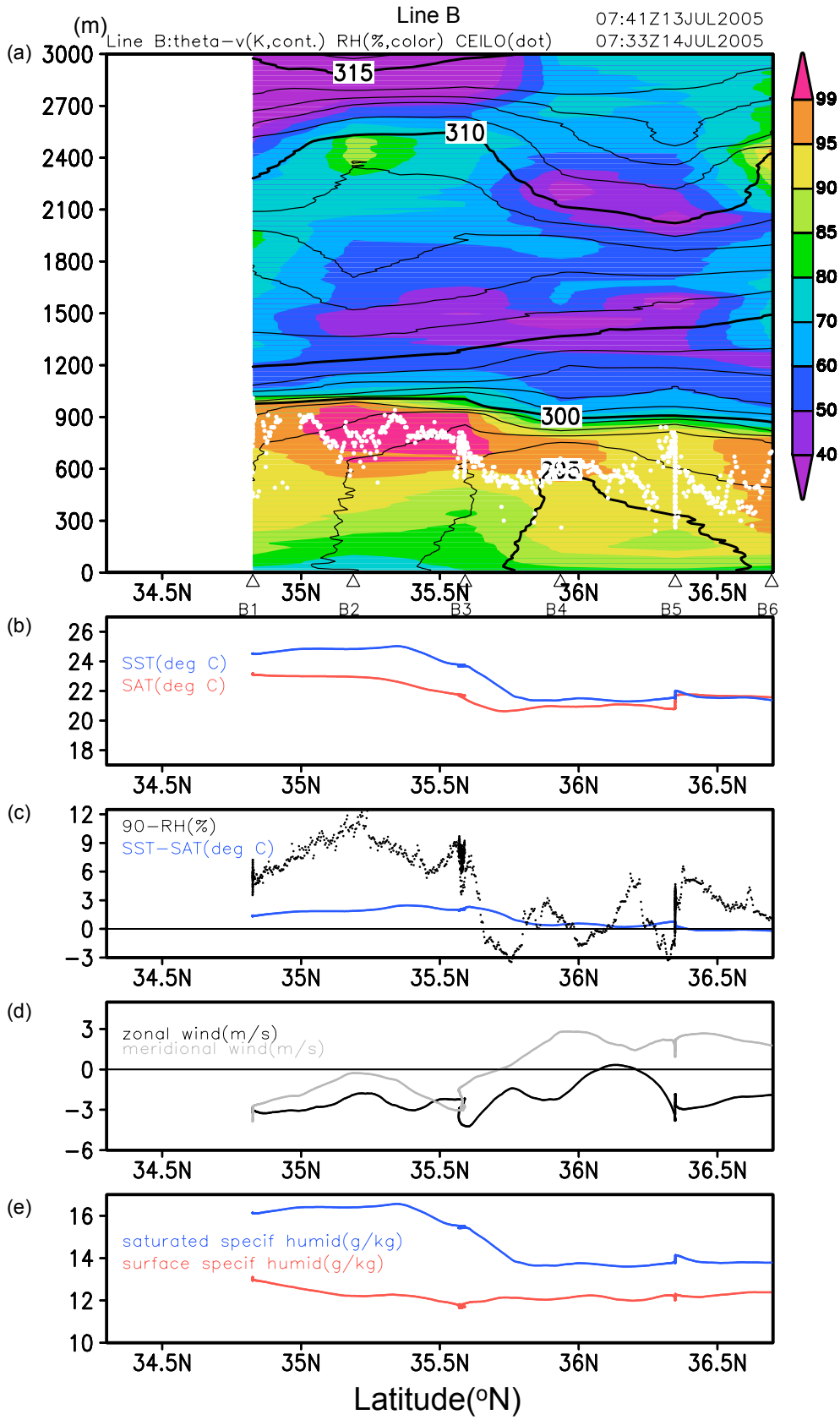

Figure 7: Same as in Fig. 4, but for Line B. Black dots in (c) represent 90 minus RH (%).

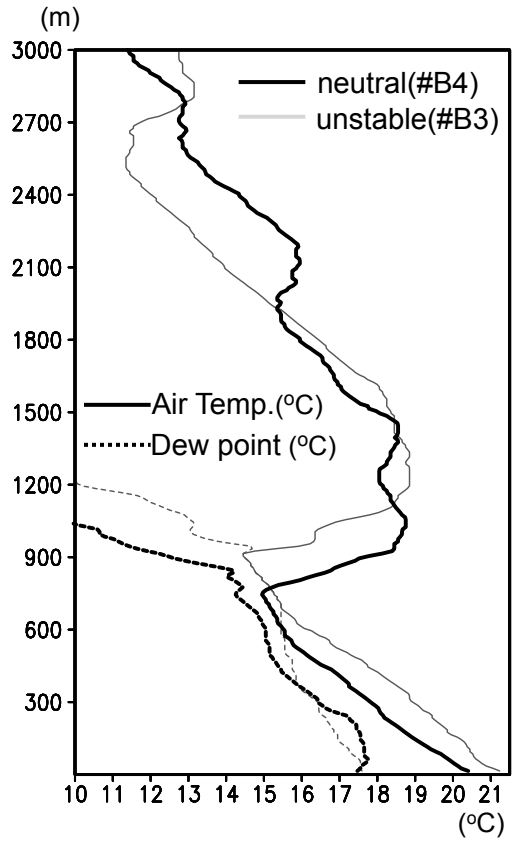

Figure 8: Same as in Fig. 5, but for Stations of B3 (gray) and B4 (black).

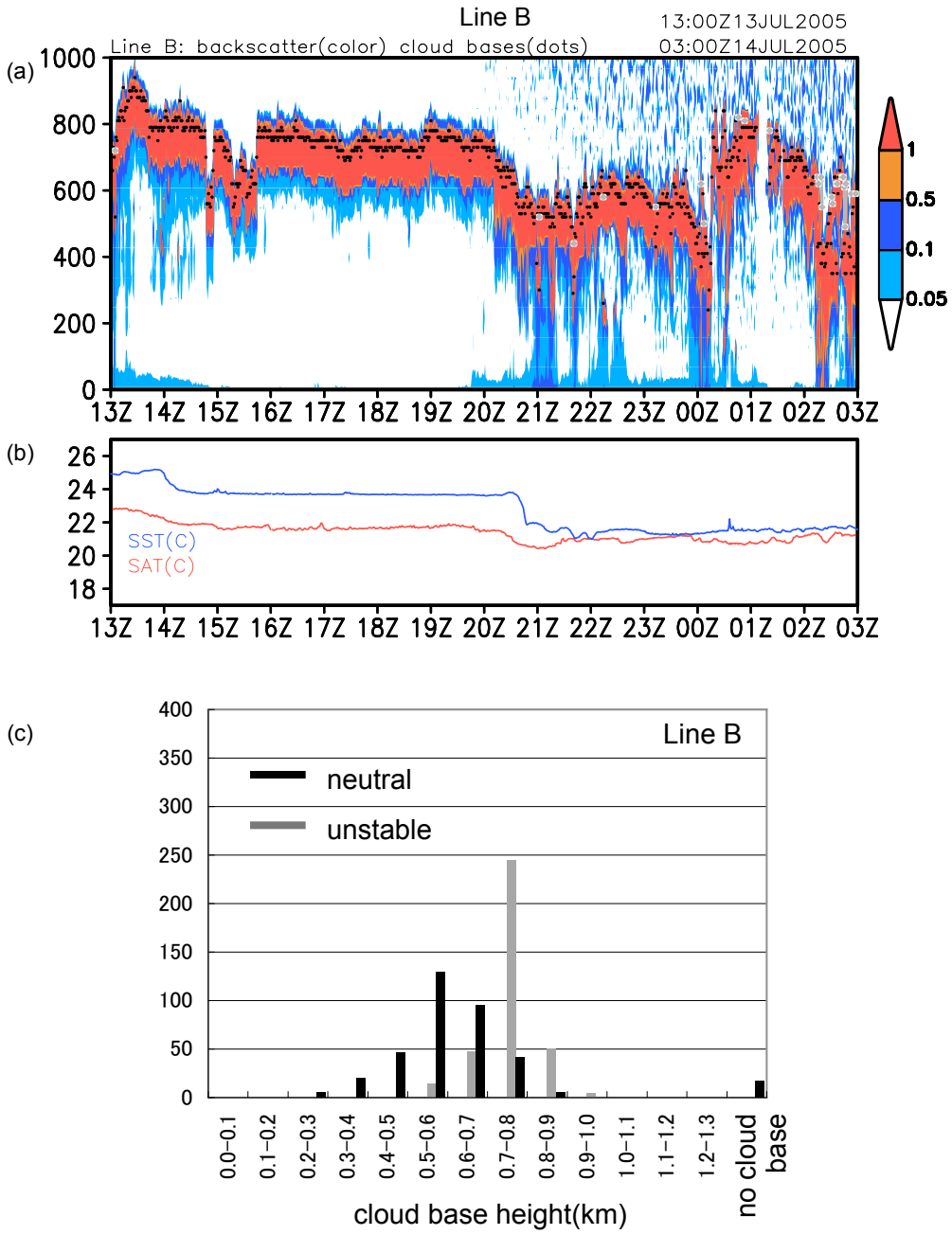

Figure 9: (a) Time-height section of ceilometer backscatter intensity [colors in 10^{-2} km^{-1} sr^{-1}] and primary cloud base (black dots). The second cloud base is plotted in gray dots when reported. (b) Time series of shipboard SST (blue in ^{o}C) and SAT (red in ^{o}C) from 1300 UTC 13 July to 0300 UTC 14 July 2005 when the ship was sailing from the warmer to colder flank of the KE SST front. (c) Same as in Fig. 6, but for Line B.

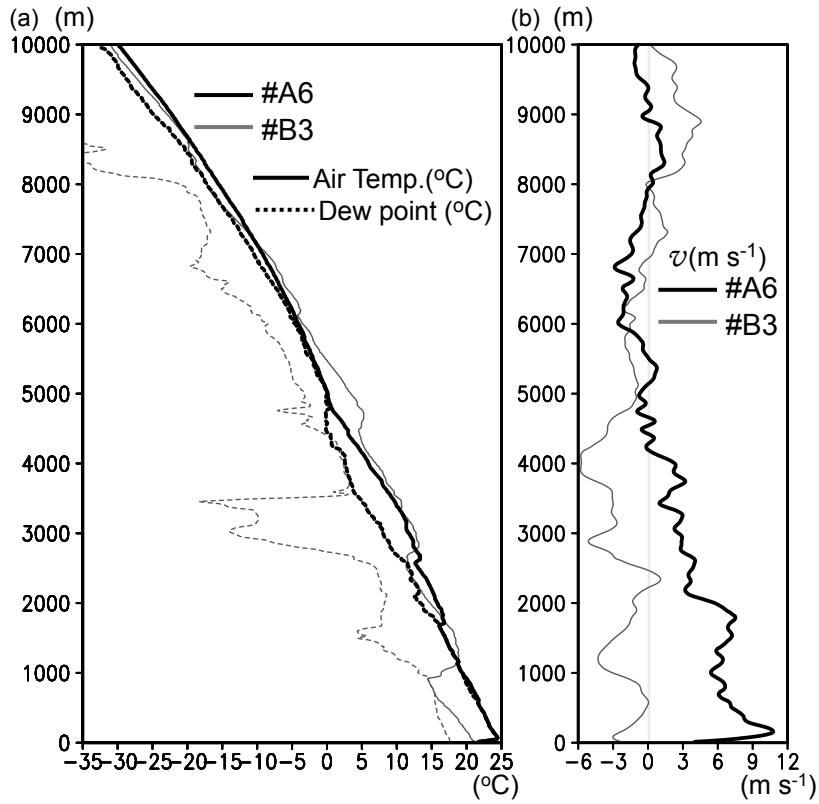

Figure 10: Vertical profiles of (a) air temperature (solid curves in °C) and dew point (dashed in °C), (b) meridional wind (solid curves in ms^{-1}) at Stations A6 (black) and B3 (gray).